Canadian Mineralogist
Vol. 27, pp. 401-418 (1989)

SILVER SULFOSALTS OF THE SANTO NIÑO VEIN, FRESNILLO DISTRICT, ZACATECAS, MEXICO

J. BRUCE GEMMELL*, HALF ZANTOP AND RICHARD W. BIRNIE
Department of Earth Sciences, Dartmouth College, Hanover, New Hampshire 03755, U.S.A.

ABSTRACT

The Santo Niño vein in the Fresnillo Ag–Pb–Zn district, Mexico, contains silver in acanthite and in the sulfosalts pyrargyrite, proustite, polybasite, selenian polybasite, tetrahedrite and stephanite, members of three silver-bearing sulfosalt solid-solution series. The sulfosalts, excepting proustite, are Sb-rich end members of their respective solid-solution series. The mineral assemblage evolved from (Cu-Ag)-bearing to Ag-bearing: a) tetrahedrite, polybasite and pyrargyrite; b) polybasite, pyrargyrite and stephanite; c) pyrargyrite and acanthite; and d) acanthite. The average sulfosalt formulas are: pyrargyrite $Ag_{3.02}(Sb_{1.00}As_{0.03})S_3$; proustite $Ag_{3.08}(Sb_{0.03}As_{0.95})S_3$; polybasite $(Ag_{15.40}Cu_{1.15})(Sb_{1.88}As_{0.19})S_{11}$; selenian polybasite $(Ag_{14.50}Cu_{1.15})(Sb_{1.92}As_{0.12})(Se_{1.85}S_{9.15})$; tetrahedrite $(Cu_{5.92}Ag_{4.21})(Fe_{1.43}Zn_{0.73})(Sb_{3.91}As_{0.11})S_{13}$; and stephanite $(Ag_{4.81}Cu_{0.13})(Sb_{1.05}As_{0.06})S_4$. Compositional tie-lines and relative semi-metal [Sb/(Sb + As)] values for coexisting pairs of pyrargyrite-polybasite, pyrargyrite–tetrahedrite, and polybasite–tetrahedrite, and for triplets of pyrargyrite–polybasite–tetrahedrite show systematic trends (pyrargyrite > tetrahedrite > polybasite) and appear to be temperature-dependent [higher temperature, lower Sb/(Sb + As) values]. Sulfosalt (Sb–As) and (Ag–Cu) patterns indicate that element substitution, not fractional crystallization, determines the semi-metal and metal variations in the silver-bearing sulfosalts of the Santo Niño vein. Pyrargyrite shows only (Sb–As) substitution, tetrahedrite shows coupled (Sb–As) and (Ag–Cu) substitution, whereas polybasite shows noncoupled (Sb–As) and (Ag–Cu) substitution. The distribution of Sb/(Sb + As) values in polybasite and of Ag/(Ag + Cu) values in tetrahedrite indicates that the ore-bearing solutions flowed from a deeper, southwestern part of the district to shallower levels in the northeast.

Keywords: sulfosalts, pyrargyrite, polybasite, tetrahedrite, stephanite, compositional tie-lines, geothermometry, paragenesis, epithermal vein, Fresnillo District, Mexico.

SOMMAIRE

Le filon de Santo Niño, dans le district minéralisé en Ag–Pb–Zn de Fresnillo, au Mexique, contient de l'argent dans l'acanthite et les sulfosels pyrargyrite, proustite, polybasite, polybasite sélénifère, tétraédrite et stéphanite, membres de trois solutions solides riches en Ag. A l'exception de la proustite, les sulfosels sont les pôles Sb de leurs séries respectives. Les assemblages ont évolués d'une composition Cu–Ag à simplement argentifère: a) tétraédrite, polybasite et pyrargyrite; b) polybasite, pyrargyrite et stéphanite; c) pyrargyrite et acanthite, et d) acanthite. Les formules moyennes sont: pyrargyrite $Ag_{3.02}(Sb_{1.00}As_{0.03})S_3$; proustite $Ag_{3.08}(Sb_{0.03}As_{0.95})S_3$; polybasite $(Ag_{15.40}Cu_{1.15})(Sb_{1.88}As_{0.19})S_{11}$; polybasite sélénifère $(Ag_{14.50}Cu_{1.15})(Sb_{1.92}As_{0.12})(Se_{1.85}S_{9.15})$; tétraédrite $(Cu_{5.92}Ag_{4.21})(Fe_{1.43}Zn_{0.73})(Sb_{3.91}As_{0.11})S_{13}$; et stéphanite $(Ag_{4.81}Cu_{0.13})(Sb_{1.05}As_{0.06})S_4$. La composition et la valeur Sb/(Sb + As) des couples pyrargyrite–polybasite, pyrargyrite-tétraédrite, polybasite–tétraédrite, et des triplets pyrargyrite–polybasite–tétraédrite, varient systématiquement (pyrargyrite > tétraédrite > polybasite) et semblent liées à la température [plus elle est élevée, plus le rapport Sb/(Sb + As) est faible]. Les relations Sb–As et Ag–Cu dans les sulfosels montrent que les exigeances des mécanismes de substitution et non la cristallisation fractionnée déterminent les variations en teneurs des métaux et semi-métaux dans les sulfosels argentifères du filon de Santo Niño. La pyrargyrite montre seulement une substitution (Sb–As), la tétraédrite, une substitution couplée (Sb–As et Ag–Cu), et la polybasite, une substitution non-couplée de Sb–As et de Ag–Cu. La distribution des valeurs de Sb/(Sb + As) dans la polybasite et de Ag/(Ag + Cu) dans la tétraédrite fait penser que les fluides responsables de la minéralisation se sont écoulés à partir d'une source profonde dans le sud-ouest vers des zones moins profondes du système dans le nord-est.

(Traduit par la Rédaction)

Mots-clés: sulfosels, pyrargyrite, polybasite, tétraédrite, stéphanite, compositions coexistantes, géothermométrie, paragenèse, filon épithermal, district de Fresnillo, Mexique.

INTRODUCTION

The Fresnillo District, located 750 km northwest of Mexico City, is a world-class silver–lead–zinc deposit that includes epithermal veins, replacement bodies in the form of mantos and chimneys, and an oxidized stockwork. The district is located in the northern part of a north-northwest-trending belt of silver–lead–zinc deposits that extends for more than 800 km and includes the mining districts of Taxco, Pachuca, Guanajuato, Zacatecas, and Sombrerete (Fig. 1). Since the mid-sixteenth century, the Fresnillo District has produced more than 10,000 t of silver, 19 t of gold, and 700,000 t each of lead and zinc (Ruvalcaba-Ruiz & Thompson 1988). Silver was discovered in the Fresnillo District in 1553, and mining

*Present address: Geology Department, University of Tasmania, GPO Box 252C, Hobart, Tasmania 7001, Australia.

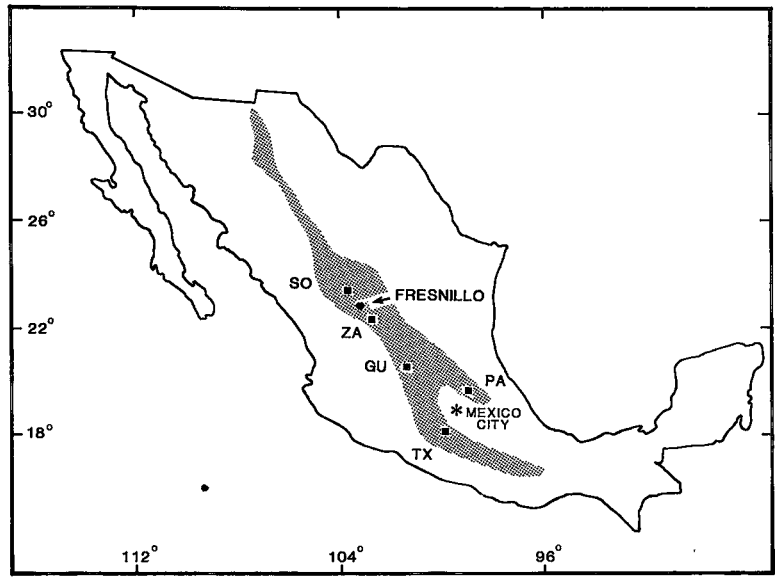

FIG. 1. Geographic location of the Fresnillo District in Mexico. Stippled area outlines belt of silver–lead–zinc deposits in central Mexico (after Damon *et al.* 1981). Abbreviations for mining districts: TX Taxco, PA Pachuca, GU Guanajuato, ZA Zacatecas, SO Sombrerete.

of the silver oxides in a near-surface stockwork began in 1554 (Church 1907, Baker 1923). Mining and milling of the sulfide ores were initiated in 1926 (Byler 1930). Reviews of the mineral deposits in the Fresnillo District are given by MacDonald *et al.* (1986), Zantop *et al.* (1986), Ruvalcaba-Ruiz & Thompson (1988), and García *et al.* (1989).

The Santo Niño vein, discovered by drilling in 1975, is located approximately 2 km southeast of the previously known veins in the district and at present is the major producer at Fresnillo. Among the several previous geological investigations and reports on the Santo Niño vein, Chico (1980) discussed the exploration strategies and discovery, Ruvalcaba-Ruiz (1980, 1983) described the geology, alteration and fluid-inclusion geochemistry of the upper levels, and Gemmell *et al.* (1985, 1988), Gemmell (1986), and Simmons (1986) described the vein geology. Simmons (1986), Simmons & Sawkins (1986), and Simmons *et al.* (1988) discussed the physicochemical conditions of the mineralizing solutions on the basis of fluid-inclusion and isotopic evidence.

One of the unusual aspects of the Santo Niño vein is the occurrence of three separate silver-bearing sulfosalt solid-solution series. In this study we sought to determine: (a) the identity and paragenesis of the sulfosalts, (b) the compositions and nature of the solid solutions in each sulfosalt series, and (c) their spatial variations throughout the vein. The scientific and practical significance of these investigations is illustrated by Birnie & Petersen (1977), Wu & Birnie (1977), Wu & Petersen (1977), and Hackbarth & Petersen (1984). Sixty-six locations throughout the vertical and lateral extent of the vein and core from drill holes between the main levels were selected for detailed mineralogical and geochemical studies. Preliminary data concerning the sulfosalt mineralogy and geochemistry were reported by Gemmell (1986) and Gemmell *et al.* (1986, 1988).

REGIONAL GEOLOGY

Tertiary felsic volcanic rocks overlie deformed Mesozoic marine sediments and submarine mafic volcanic rocks in the Fresnillo District. Arenas (1860), Stone (1941), Stone & McCarthy (1948), DeCserna (1976), Gemmell *et al.* (1988) and García *et al.* (1989) described the geology and stratigraphy of the district. The stratigraphic sequence and distribution of rock units in the Fresnillo District (Fig. 2) consist of Lower Cretaceous greywackes and shales (Proaño Group), overlain conformably by basaltic pillow lavas, breccias and intercalated sediments (Chilitos Formation), which in turn are unconformably overlain by a Tertiary continental conglomerate and arkosic sediments (Fresnillo Formation), rhyolite tuffs and pyroclastic flows, and isolated flows of olivine basalt. The total package of sedimentary and volcanic rocks has an aggregate thickness of greater than 2700 m. An Oligocene

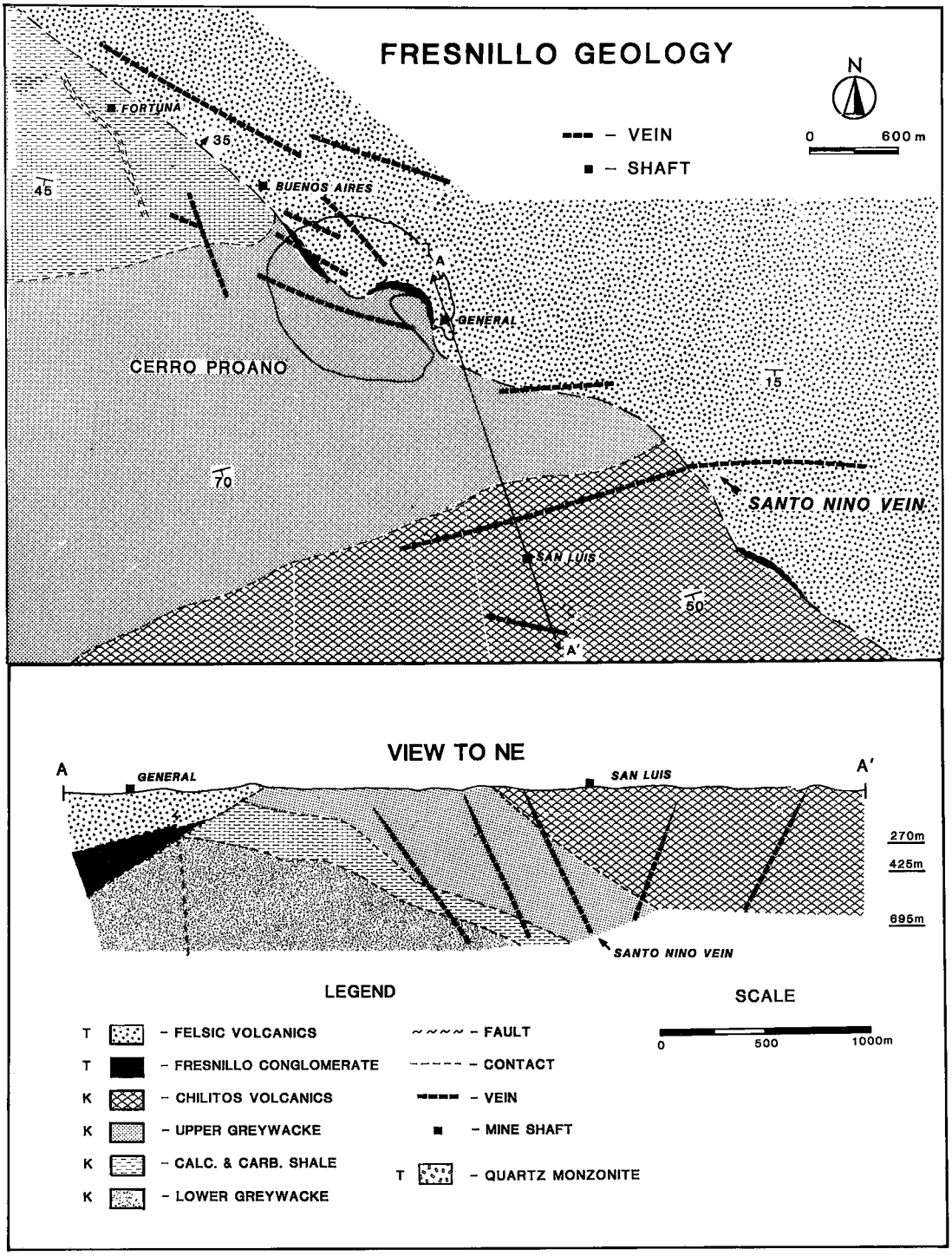

FIG. 2. Simplified geological map and cross section of the Fresnillo District showing location of the Santo Niño vein in relation to other major epithermal veins within the district. Symbols: T Tertiary, K Cretaceous.

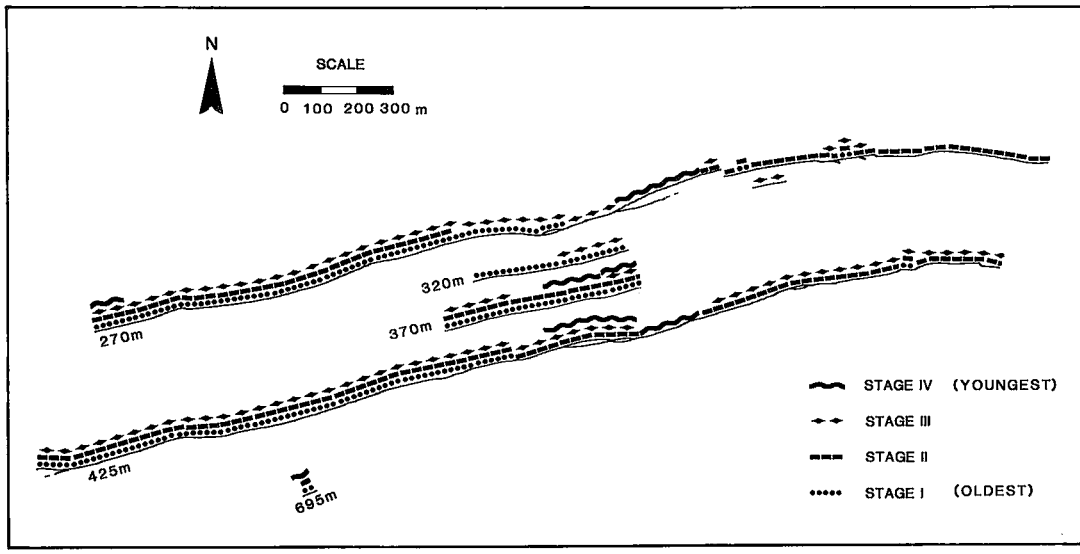

FIG. 3. Distribution of depositional stages in a plan view of the Santo Niño vein. Each symbol represents the distribution of that particular stage throughout the vein. Geological characteristics of each stage are discussed in the text.

quartz monzonite stock and younger rhyolite dykes cut the Cretaceous and Tertiary sedimentary and volcanic section.

The structure of the Fresnillo District is controlled by two separate deformational events that occurred during the Late Cretaceous and Middle to Late Tertiary. Within the Proaño Group sediments, a broad anticlinorium plunging gently to the southeast below Cerro Proaño (Fig. 2) reveals crumpling and contortion, which resulted from Late Cretaceous folding and associated thrust faulting. Block faulting, which caused a regional, southward tilt of the Cretaceous sequence and the overlying Tertiary continental sedimentary and volcanic rocks, occurred in the Middle to Late Tertiary. The most prominent example of this deformation in the mine area is the Fresnillo fault, which brings the Fresnillo Formation and Tertiary felsic volcanic rocks into contact with the underlying Upper Greywacke unit and Chilitos Formation (Fig. 2). Extensive development of minor tensional faults and fractures followed and coincided with the hydrothermal activity that resulted in the vein mineralization described in this paper.

GEOLOGY OF THE SANTO NIÑO VEIN

The Santo Niño vein trends N 70°E, dips 60° to 80°SE, has a strike length of greater than 2.5 km, and a vertical extent of greater than 500 m. Vein width ranges from less than 10 cm to greater than 4 m, and average 2.5 m. The Santo Niño vein has proven reserves of 1.2 million tonnes grading at 769 g/ton Ag, 0.56 g/ton Au, 0.99% Zn, 0.50% Pb, and 0.03% Cu (García *et al.* 1989). Host rocks for the vein are greywackes and shales of the Cretaceous Upper Greywacke unit, mafic volcanic rocks of the Cretaceous Chilitos Formation, and a conglomerate of the Tertiary Fresnillo Formation. The age of mineral deposition is Eocene–Oligocene (Lang *et al.* 1988).

The Santo Niño vein can be divided into three structural zones, all of which are related to oblique deformation with dominant right-lateral strike-slip. Total lateral displacement seems to have been only a few meters. The western structural zone is characterized by a linear strike with pinching and swelling, the central structural zone by cymoid loops, and the eastern structural zone by right-stepping *en échelon* segments. Four separate stages of vein formation record the multiple openings of fissures that provided a conduit for hydrothermal solutions responsible for the mineral deposition in the vein (Fig. 3). Stage I is divided into a crackle breccia found adjacent to the footwall contact and a fragment-to-matrix supported breccia containing unaltered fragments, well-developed cockade layering of sulfides and quartz, and a matrix of white and grey quartz. Stage II is predominantly a fragment-supported breccia with highly altered fragments, poorly developed cockade layering with minor sulfides, and a distinct chlorite-rich, green-tinted quartz matrix. Stage III consists of crustiform layers of quartz and sulfides. Stage IV is a massive flooding of coarsely crystalline calcite. Stage I contains the greatest amount of ore within the vein, followed by Stages III, II, and IV.

Hydrothermal alteration is generally weakly devel-

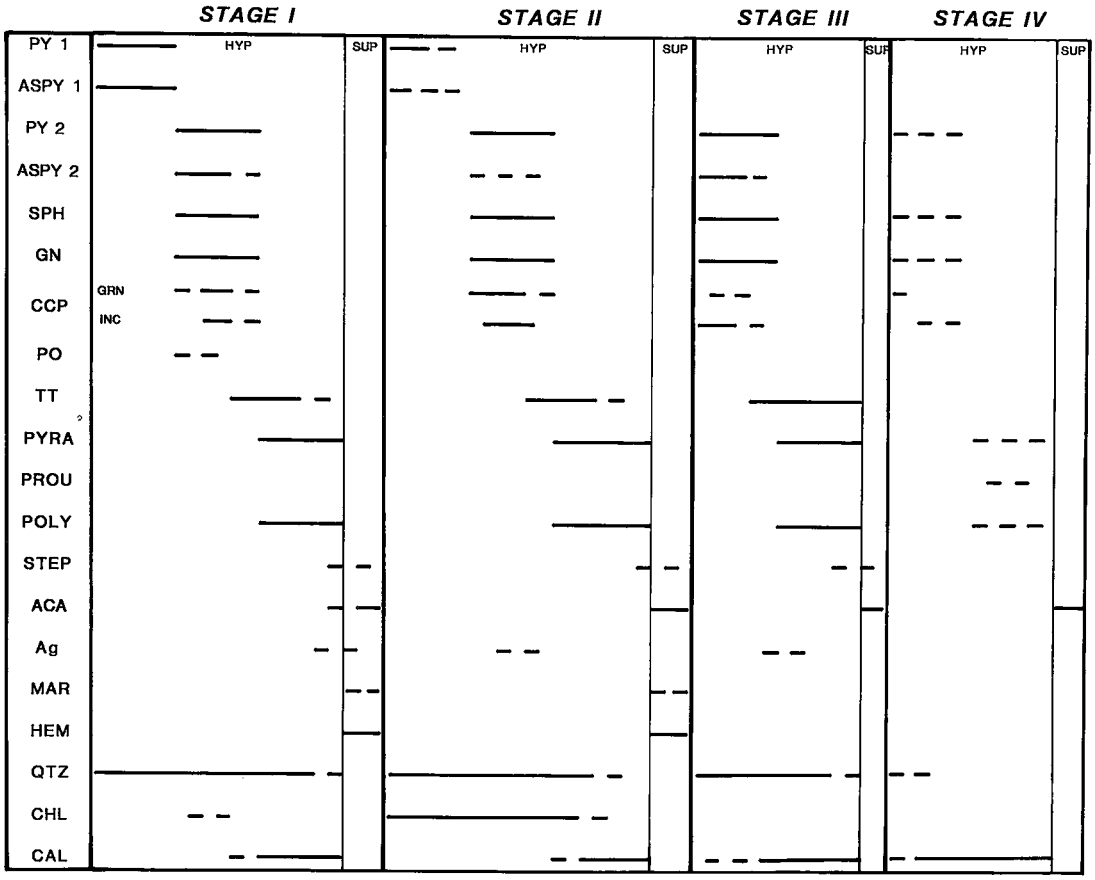

FIG. 4. Paragenetic sequence of ore and gangue mineral deposition in Stages I through IV. Dashed line indicates trace amounts. Abbreviations: PY pyrite, ASPY arsenopyrite, SPH sphalerite, GN galena, CCP chalcopyrite, PO pyrrhotite, TT tetrahedrite, PYRA pyrargyrite, PROU proustite, POLY polybasite, STEP stephanite, ACA acanthite, Ag native silver, MAR marcasite, HEM hematite, QTZ quartz, CHL chlorite, CAL calcite, GRN grains, INC inclusions, HYP hypogene minerals, and SUP supergene minerals.

oped around the veins in the Fresnillo District and rarely extends more than a few meters away from the veins. The types of alteration observed in the wallrocks are propylitization of the volcanic rocks of the Chilitos Formation and silicification of the sediments of the Upper Greywacke unit. Conglomerates of the Fresnillo Formation contain both silicification and weak propylitic alteration. Silicification, argillization, and propylitization of fragments in the breccia stages are observed in the Santo Niño vein.

SULFIDE AND SULFOSALT MINERALOGY AND PARAGENESIS

The ore minerals of the Santo Niño vein are a complex intergrowth of fine-grained base metal sulfides and silver-bearing sulfosalts. In order of abundance, these are pyrite, sphalerite, galena, pyrargyrite, polybasite, chalcopyrite, arsenopyrite, tetrahedrite, acanthite, stephanite, marcasite, proustite, pyrrhotite, and selenian polybasite. The ratio of sulfide to sulfosalt is approximately 5:1, with sulfides and sulfosalts making up less than 5% by volume of the vein. Gangue minerals include quartz, chalcedony, calcite, chlorite, and several clay-mineral species (montmorillonite, kaolinite, mixed-layer chlorite–smectite, and trace amounts of illite or sericite). The ore and gangue minerals occur as crustified layers, cockade textures, disseminations and stringers within breccia matrix, and replacement of breccia fragments. Oxidized fractures contain limonite, hematite, Mn oxide, malachite, azurite, and native silver.

Mineral deposition is divided into four paragenetic phases: 1) pyrite and arsenopyrite, 2) sphalerite,

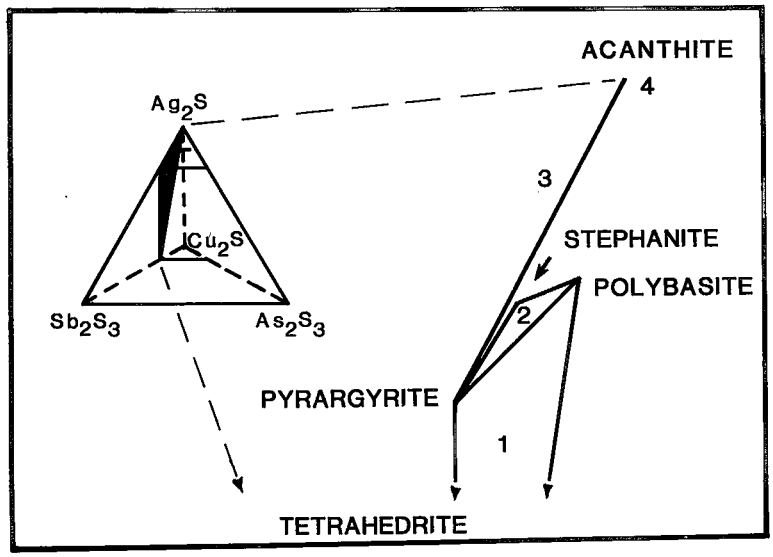

FIG. 5. Paragenesis of the silver-bearing sulfides and sulfosalts of the Santo Niño vein within the quaternary system Ag_2S–Sb_2S_3–As_2S_3–Cu_2S. The numbers indicate the sequence of minerals corresponding to precipitation from the systems [(Cu,Ag) (Fe,Zn)–Sb–S; Cu–Ag–Sb–S, Ag–Sb–S], [Cu–Ag–Sb–S; Ag–Sb–S], [Ag–Sb–S; Ag–S], and [Ag–S]. The diagram is generalized because members of the tetrahedrite–tennantite series have a slight excess in sulfur (1 of 13 atoms) and do not plot precisely on the Sb_2S_3–As_2S_3–Cu_2S plane.

galena, and chalcopyrite, with a second generation of pyrite and arsenopyrite, 3) silver-bearing sulfosalts and sulfides, and 4) supergene sulfides and oxides. The paragenetic sequence of the ore and gangue minerals for each stage of the Santo Niño vein is similar (Fig. 4).

The paragenetic evolution of the silver-bearing sulfosalt and sulfide minerals is from (copper–silver)-bearing to pure silver-bearing: a) tetrahedrite, polybasite, and pyrargyrite, b) polybasite, pyrargyrite, and stephanite, c) pyrargyrite and acanthite, and d) acanthite. This paragenesis of the silver-bearing minerals within the Ag_2S–Sb_2S_3–As_2S_3–Cu_2S quaternary system is shown in Figure 5. Tetrahedrite was the first sulfosalt to precipitate, initially with chalcopyrite and subsequently with pyrargyrite and polybasite. Complex symplectitic intergrowths of pyrargyrite, polybasite, tetrahedrite, chalcopyrite, and galena are beautifully developed (Figs. 6a,b). Pyrargyrite and polybasite replaced earlier generations of sulfides and tetrahedrite. Pyrargyrite and polybasite commonly fill tiny fractures and cracks in other ore minerals, and rarely fill voids between crystals of late-stage euhedral quartz and calcite gangue. Trace quantities of stephanite are associated with polybasite, as a pseudomorphic replacement. Minor amounts of acanthite are intergrown with the silver-bearing sulfosalts, mainly late-stage pyrargyrite.

COMPOSITION OF THE SULFOSALTS

The Santo Niño vein contains three separate silver-bearing sulfosalt solid-solution series: pyrargyrite–proustite [$Ag_3(Sb,As)S_3$], polybasite–arsenpolybasite [$(Ag,Cu)_{16}(Sb,As)_2S_{11}$], and tetrahedrite–tennantite [$(Cu,Ag)_{12}(Sb,As)_4S_{13}$]. Stephanite ($Ag_5SbS_4$) is observed, but does not form a solid-solution series with an arsenic analog.

Compositions were determined by electron-microprobe analysis from samples selected to

FIG. 6. Microphotographs of sulfosalt mineral textures in the Santo Niño vein. (a) Symplectitic intergrowth of galena (GN) and pyrargyrite (PYRA) enveloped by polybasite (POLY). Black grains are gangue. Stage I, oil; (b) Symplectitic intergrowth of tetrahedrite (TT) and galena (GN) surrounded by pyrargyrite (PYRA) and sphalerite riddled with inclusions of chalcopyrite. Black grains are quartz. Stage III, air; c) Intergrowth of coexisting polybasite (POLY), tetrahedrite (TT), and pyrargyrite (PR). Sulfosalts precipitated after cockscomb quartz crystals (black, hexagonal crystal outline) and minor amounts of pyrite (PY), galena (GN), and sphalerite (SPH). Sphalerite is riddled with tiny inclusions of chalcopyrite. Stage I, oil.

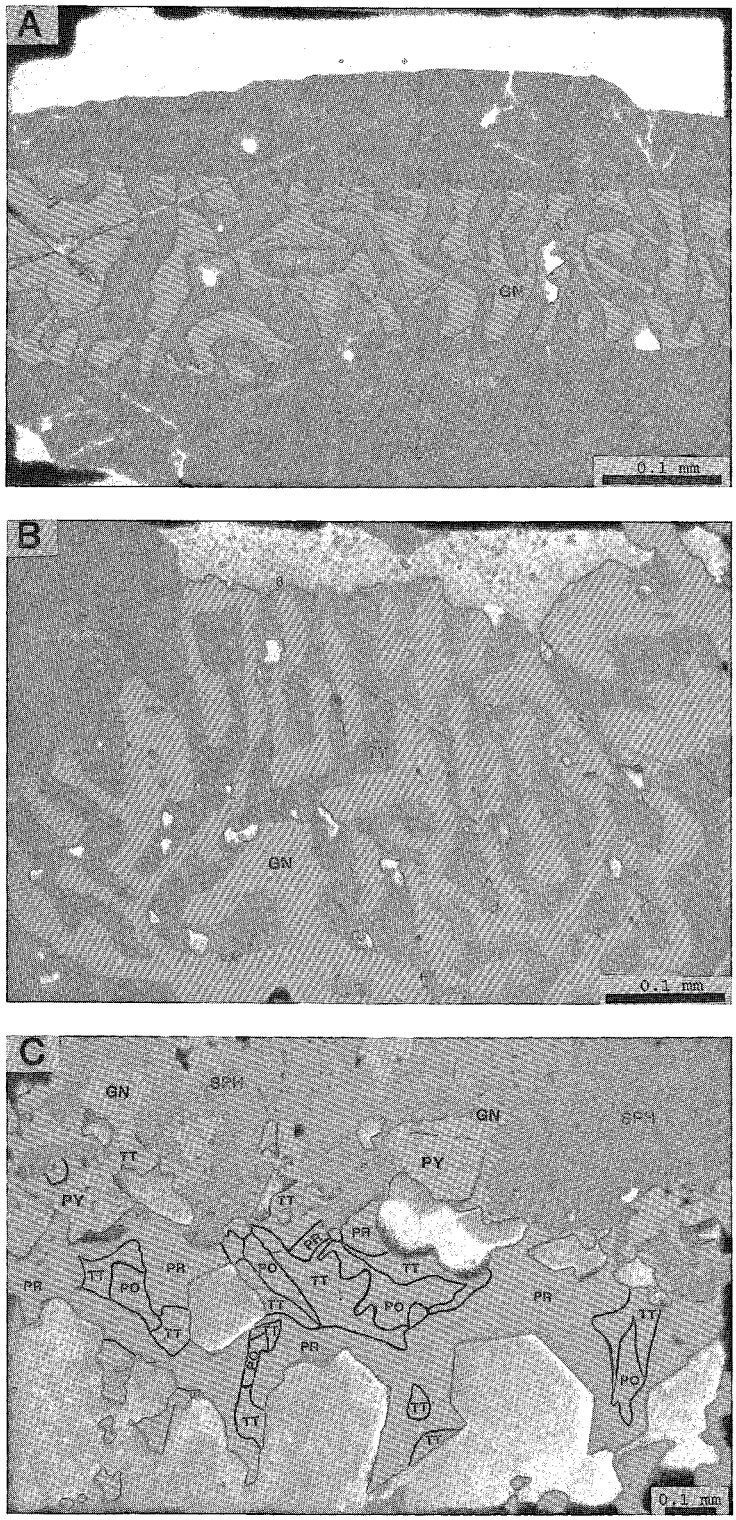
A
GN
0.1 mm
B
GN
0.1 mm
C
GN
GN
PY
PY
TT
PR
PO
0.1 mm

TABLE 1. SULFOSALT ANALYTICAL PARAMETERS

MINERAL	ELEMENT	SPECTRAL LINE	CRYSTAL	DETECTION (Wt.%)	PRECISION (±Wt.%)
PYRARGYRITE	Ag	L	PET	0.03	0.41
	Cu	K	LIF	0.03	0.01
	Sb	L	PET	0.03	0.20
	As	K	LIF	0.06	0.03
	S	K	PET	0.01	0.11
POLYBASITE	Ag	L	PET	0.04	0.50
	Cu	K	LIF	0.03	0.04
	Sb	L	PET	0.03	0.12
	As	K	LIF	0.05	0.03
	S	K	PET	0.01	0.10
TETRAHEDRITE	Ag	L	PET	0.03	0.23
	Cu	K	LIF	0.02	0.14
	Zn	K	LIF	0.03	0.04
	Fe	K	LIF	0.02	0.04
	Pb	M	PET	0.06	0.04
	Sb	L	PET	0.04	0.20
	As	K	LIF	0.05	0.03
	S	K	PET	0.01	0.13
STEPHANITE	Ag	L	PET	0.04	0.46
	Cu	K	LIF	0.02	0.02
	Sb	L	PET	0.03	0.16
	As	K	LIF	0.05	0.03
	S	K	PET	0.01	0.10

Data obtained with a Cameca MXB electron microprobe automated with a Tracor Northern TN-2000/1310 system interfaced through a DEC PDP-11/04 microcomputer. An accelerating potential of 25 kV with a nominal beam current of 15 nA was used for all analyses. Synthetic pyrargyrite, proustite, tetrahedrite, and galena were used as standards and the data corrected for differential matrix effects by the ZAF program of Doyle & Chambers (1981).

represent all four stages of vein formation over the vertical and lateral extent of the vein. Analytical procedures and parameters, which are similar to those outlined by Hackbarth & Petersen (1984), are listed in Table 1. Because of the large volume of compositional data, three tables of data (Table A for pyrargyrite–proustite; Table B for polybasite; Table C for stephanite–tetrahedrite) have been submitted to the Depository of Unpublished Data, CISTI, National Research Council of Canada, Ottawa, Ontario K1A 0S2. Summaries of the sulfosalt compositional data are given in Tables 2–5.

Pyrargyrite – proustite

Pyrargyrite is the most abundant sulfosalt in the vein. Relevant compositional data, and data for proustite, are given in Table 2. These data indicate that the composition of pyrargyrite in the four stages of the vein throughout its entire vertical and lateral extent is relatively constant, with a mean composition corresponding to $Ag_{3.02}(Sb_{1.00}As_{0.03})S_3$. Traverses of several pyrargyrite grains showed no systematic chemical variation or zoning.

Three pyrargyrite grains have intermediate compositions in the solid-solution series. Antimony and arsenic concentrations are the main variables: $Ag_{2.95}(Sb_{0.72}As_{0.29})S_3$, $Ag_{3.17}(Sb_{0.59}As_{0.46})S_3$, and $Ag_{3.35}(Sb_{0.39}As_{0.59})S_3$, respectively. Two grains were identified as proustite, and both have similar compositions. Their mean composition is $Ag_{3.08}(Sb_{0.03}As_{0.95})S_3$.

Toulmin (1963) determined that pyrargyrite–proustite forms a complete solid-solution from solidus temperatures down to 300°C, but that a miscibility gap may exist below 300°C, as the composition of natural samples of ruby silver is restricted to within 17 formula % of the end members. Keighin & Honea (1969) determined that most natural samples of pyrargyrite contain small amounts of arsenic; intermediate members of the solid-solution series, however, do not seem to have been described in nature. As the temperature of mineral deposition in the Santo Niño vein, based on fluid-inclusion measurements on quartz, calcite, and sphalerite, ranges from 180 to 260°C (Simmons & Sawkins 1986), it appears that the previously postulated miscibility gap in the pyrargyrite–proustite solid solution below about 300°C (Toulmin 1963) either does not exist or begins below a temperature of 260°C.

TABLE 2. PYRARGYRITE-PROUSTITE COMPOSITION DATA

VEIN STAGE		# of analyses	Ag wt. %	Cu wt. %	Sb wt. %	As wt. %	S wt. %	TOTAL
PYRARGYRITE								
OVERALL	*MEAN*	100	59.18	0.06	22.12	0.35	17.49	99.19
	STD. DEV.		0.58	0.06	0.55	0.19	0.32	
I	*MEAN*	45	59.27	0.05	22.18	0.36	17.44	99.30
	STD. DEV.		0.53	0.06	0.44	0.21	0.30	
II	*MEAN*	40	59.18	0.06	21.98	0.36	17.46	99.03
	STD. DEV.		0.73	0.05	0.66	0.20	0.34	
III	*MEAN*	12	59.13	0.04	21.91	0.39	17.54	99.00
	STD. DEV.		0.22	0.01	0.33	0.17	0.20	
IV	*MEAN*	3	59.95	0.17	21.80	0.23	17.30	99.44
	STD. DEV.		0.27	0.16	0.96	0.15	0.35	
INTERMEDIATE COMPOSITIONS								
		1	64.33	0.29	8.39	7.90	17.10	98.01
		1	62.83	0.01	13.09	6.37	17.66	99.96
		1	60.48	0.01	16.72	4.06	18.28	99.55
PROUSTITE								
	MEAN	2	65.19	0.00	0.72	14.01	18.89	98.81

TABLE 3. POLYBASITE COMPOSITION DATA

VEIN STAGE		# of analyses	Ag wt. %	Cu wt. %	Sb wt. %	As wt. %	S wt. %	Se wt. %	TOTAL
POLYBASITE									
OVERALL	*MEAN*	66	70.59	3.11	9.75	0.60	14.99	---	99.04
	STD. DEV.		1.77	0.92	0.88	0.28	0.76	---	
I	*MEAN*	35	70.66	2.96	9.86	0.63	15.02	---	99.13
	STD. DEV.		1.91	0.94	0.92	0.22	0.82	---	
II	*MEAN*	23	70.19	3.59	9.52	0.65	15.08	---	99.03
	STD. DEV.		1.49	0.87	0.84	0.38	0.52	---	
III	*MEAN*	6	70.88	2.81	9.93	0.40	14.83	---	98.85
	STD. DEV.		1.98	0.68	0.86	0.20	1.04	---	
IV	*MEAN*	2	69.73	3.55	9.99	0.40	15.19	---	98.85
SELENIAN POLYBASITE									
		1	68.02	3.14	10.01	0.41	12.51	6.24	99.01
"ANTIMONPEARCEITE"									
	MEAN	3	64.36	9.06	9.49	0.72	15.27	---	98.89
	STD. DEV.		1.37	0.76	0.57	0.34	0.66	---	

--- = below detection limit

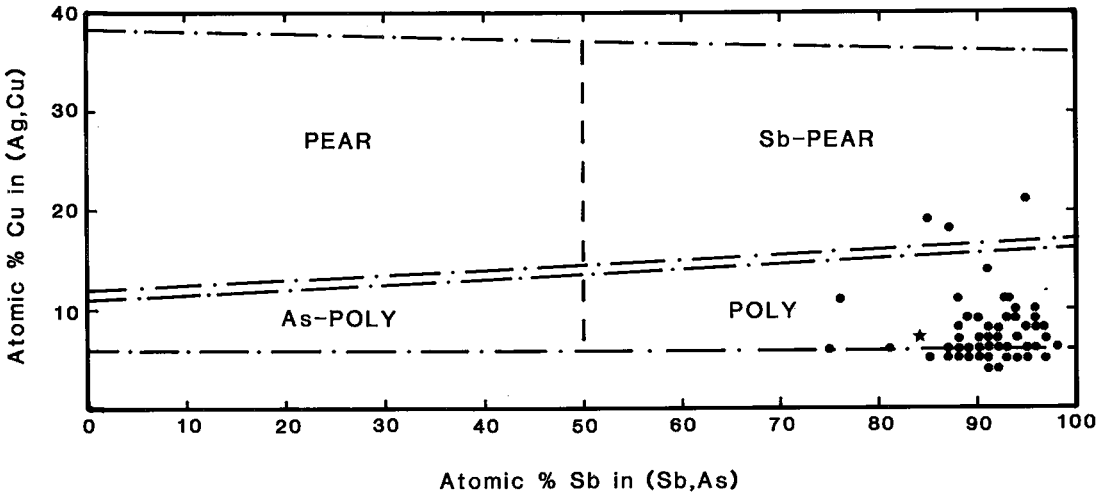

FIG. 7. Classification scheme based on compositional ranges, for polybasite (POLY)–arsenpolybasite (As-POLY) and antimonpearceite (Sb-PEAR)–pearceite (PEAR) solid-solution series (after Hall 1967). Dots indicate compositions of polybasite–arsenpolybasite from the Santo Niño vein. Star denotes selenium-rich polybasite.

Polybasite–arsenpolybasite

Polybasite–arsenpolybasite is the second most abundant solid-solution series. Relevant compositional data are given in Table 3. Polybasite and pearceite have been regarded as the antimony and arsenic end-members of a single solid-solution series (Palache *et al.* 1944, Frondel 1963). Peacock & Berry (1947), Frondel (1963) and Hall (1967) determined that there is not a continuous chemical variation from polybasite to pearceite, and suggested that polybasite–arsenpolybasite and pearceite–antimonpearceite form separate solid-solution series and that the series are isodimorphous.

Hall (1965) determined that polybasite, in synthetic systems at 200°C, contains from 3.1 to 7.6 wt.% Cu, whereas antimonpearceite has a copper content that ranges from 7.9 to 19.2 wt.%. He concluded that the limits of substitution of copper in the polybasite and pearceite synthetic series correspond closely to those in naturally occurring minerals. A classification scheme based on composition was devised by Hall (1967) to separate the polybasite–arsenpolybasite and pearceite–antimonpearceite series. Based on this classification, all but three of the Santo Niño samples consist of polybasite (Fig. 7). Their mean composition (Table 3) is $(Ag_{15.40}Cu_{1.15})(Sb_{1.88}As_{0.19})S_{11}$. The compositions of polybasite from the four stages of vein formation all span a similar range.

One grain of polybasite contains a significant amount of selenium and corresponds to $(Ag_{14.50}Cu_{1.15})(Sb_{1.92}As_{0.12})(Se_{1.85}S_{9.15})$. Selenian polybasite is very rare (Harris *et al.* 1965). Motomura & Yamamoto (1980) compiled all of the known occurrences of selenium-bearing members of the polybasite and pearceite groups. The selenium-rich polybasite from the Santo Niño vein has a composition similar to that of other examples of selenium-rich polybasite from a variety of vein deposits around the world.

Three grains plot in the "antimonpearceite" field (Fig. 7), and their mean composition is

TABLE 4. STEPHANITE COMPOSITION DATA

VEIN STAGE		# of analyses	Ag wt. %	Cu wt. %	Sb wt. %	As wt. %	S wt. %	TOTAL
STEPHANITE								
OVERALL	*MEAN*	10	65.25	1.03	16.08	0.60	16.14	99.09
	STD. DEV.		1.96	0.74	1.33	0.49	0.47	
I	*MEAN*	5	65.12	1.55	16.07	0.51	16.22	99.47
	STD. DEV.		2.11	0.47	1.71	0.17	0.55	
II	*MEAN*	3	65.07	0.73	16.06	0.92	16.34	99.12
	STD. DEV.		2.51	0.69	1.12	0.86	0.28	
III	*MEAN*	2	65.81	0.19	16.13	0.34	15.64	98.10
	STD. DEV.		1.82	0.27	1.77	0.23	0.06	

TABLE 5. TETRAHEDRITE COMPOSITION DATA

VEIN STAGE		# of analyses	Ag wt. %	Cu wt. %	Zn wt. %	Fe wt. %	Pb wt. %	Sb wt. %	As wt. %	S wt. %	TOTAL
TETRAHEDRITE											
OVERALL	*MEAN*	23	24.25	20.08	2.56	4.26	0.13	25.36	0.45	22.23	99.31
	STD. DEV.		5.89	4.37	0.98	1.36	0.09	1.73	0.28	1.21	
I	*MEAN*	6	21.19	22.47	3.16	3.48	0.12	25.57	0.45	22.44	98.89
	STD. DEV.		3.05	2.09	1.25	1.00	0.02	0.30	0.21	0.46	
II	*MEAN*	14	22.55	21.48	2.56	5.06	0.12	24.19	0.56	22.62	99.14
	STD. DEV.		7.61	5.45	6.74	2.29	0.03	1.73	0.26	2.01	
III	*MEAN*	3	23.75	20.86	2.95	3.69	0.24	25.18	0.57	22.38	99.62
	STD. DEV.		0.20	0.19	0.37	0.17	0.24	1.59	0.07	0.1	

TABLE 6. SULFOSALT SEMI-METAL and METAL RATIOS

		Sb/(Sb+As)				Ag/(Ag+Cu)				
MINERAL	STAGE	N	RANGE	MEAN	STD. DEV.	STAGE	N	RANGE	MEAN	STD. DEV.
PYRARGYRITE	overall	100	0.93 - 1.00	0.97	0.01	overall	100	0.99 - 1.00	1.00	0.00
	I	45	0.93 - 0.99	0.97	0.02	I	45	0.99 - 1.00	1.00	0.00
	II	40	0.95 - 1.00	0.98	0.01	II	40	0.99 - 1.00	1.00	0.00
	III	12	0.94 - 0.99	0.97	0.01	III	12	1.00	1.00	NA
	IV	3	0.97 - 0.99	0.98	0.01	IV	3	0.99 - 1.00	1.00	0.01
INTERMEDIATE COMPOSITIONS	I	1	0.56	NA	NA	I	1	1.00	NA	NA
	III	2	0.72, 0.40	NA	NA	III	2	0.99, 1.00	NA	NA
PROUSTITE	IV	2	0.02, 0.03	NA	NA	IV	2	1.00	NA	NA
POLYBASITE	overall	66	0.75 - 0.97	0.91	0.04	overall	66	0.79 - 0.96	0.93	0.02
	I	35	0.81 - 0.97	0.9	0.03	I	35	0.86 - 0.96	0.93	0.02
	II	22	0.75 - 0.97	0.90	0.06	II	22	0.89 - 0.95	0.92	0.02
	III	7	0.89 - 0.97	0.94	0.03	III	7	0.91 - 0.96	0.94	0.02
	IV	2	0.96, 0.92	NA	NA	IV	2	0.92	NA	NA
ANTIMONPEARCEITE	II	3	0.85 - 0.95	0.89	0.05	III	3	0.79-0.82	0.81	0.02
STEPHANITE	overall	10	0.85 - 0.98	0.94	0.04	overall	11	0.95 - 1.00	0.97	0.02
	I	5	0.92 - 0.97	0.95	0.02	I	6	0.95 - 0.98	0.96	0.01
	II	3	0.85 - 0.97	0.92	0.07	II	3	0.96 - 1.00	0.98	0.02
	III	2	0.95, 0.98	NA	NA	III	2	0.99 - 1.00	NA	NA
TETRAHEDRITE	overall	23	0.93 - 1.00	0.97	0.02	overall	23	0.21 - 0.58	0.42	0.11
	I	6	0.95 - 0.98	0.97	0.01	I	6	0.32 - 0.46	0.36	0.06
	II	14	0.94 - 1.00	0.97	0.02	II	14	0.21 - 0.58	0.45	0.13
	III	3	0.96 - 0.97	0.96	0.01	III	3	0.39	0.39	NA

Ratios calculated from atomic percent from data in Depository Tables A-C. NA - Not Applicable.

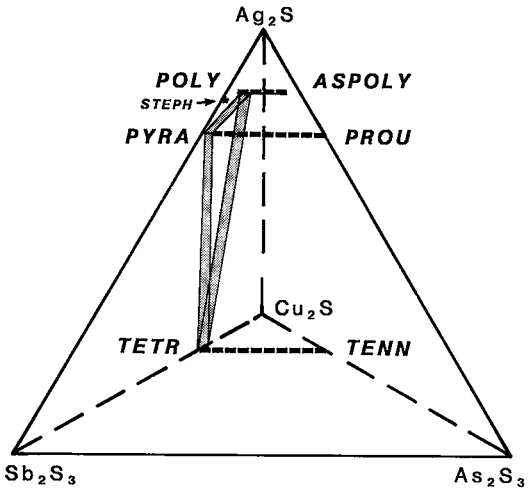

FIG. 8. Compositional range of the sulfosalt minerals in the Santo Niño vein in terms of the system Ag_2S–Sb_2S_3–As_2S_3–Cu_2S. Total range of Sb/(Sb+As) for each sulfosalt solid-solution series plotted for reference.

$(Ag_{13.78}Cu_{3.29})(Sb_{1.79}As_{0.22})S_{11}$. The compositional data for these three grains (Table 3) indicate that the silver content is lower and the copper content is higher than in polybasite. Unfortunately, our material is not suited for X-ray powder analysis; therefore, we cannot positively identify these grains as being antimonpearceite.

Stephanite

Stephanite is a minor phase throughout the vein

The sulfosalts of the Santo Niño vein have compositions that are antimony-rich and lie near the Ag_2S–Cu_2S–Sb_2S_3 plane of the Ag_2S–Sb_2S_3–As_2S_3–Cu_2S quaternary diagram. Abbreviations: POLY polybasite, ASPOLY arsenpolybasite, PYRA pyrargyrite, PROU proustite, STEPH stephanite, TETR tetrahedrite, TENN tennantite. The diagram is generalized because tetrahedrite-tennantite compositions have a slight excess in sulfur (1 of 13 atoms) and do not plot precisely on the Sb_2S_3–As_2S_3–Cu_2S plane.

system, with a mean composition (Table 4) of $(Ag_{4.81}Cu_{0.13})(Sb_{1.05}As_{0.06})S_4$. Stephanite grains from Stages I, II and III have similar compositions. Although copper is not a normal component of the stephanite structure, minor amounts of copper (up to 2.03 wt.% recorded in stephanite from the Santo Niño vein may have been incorporated during replacement of pre-existing polybasite by stephanite (Gemmell *et al.* 1988). Similarly, stephanite does not normally form a solid-solution series with an arsenic analog, and the arsenic values of 0.17 to 1.88 wt.% may be inherited from polybasite replacement as well.

Keighin & Honea (1969) discovered that heating a sample of stephanite to 197 ±5°C at 1 bar causes it to break down to pyrargyrite plus argentite, suggesting that 197°C represents the maximum temperature of deposition of the stephanite. In the case of the Santo Niño vein, the presence of stephanite indicates that the temperature of the hydrothermal fluid was lower than 197°C (estimated pressure during mineral precipitation was 15 – 60 bars, as discussed by Simmons *et al.* 1988) when the stephanite precipitated, which is near the lower end of the fluid-inclusion temperatures reported by Simmons & Sawkins (1986). This conclusion is supported by the fact that stephanite forms as a hypogene mineral very late in the paragenetic sequence.

Tetrahedrite–tennantite

Tetrahedrite–tennantite is the least abundant solid-solution series in the Santo Niño vein. Tetrahedrite is the only member present in the vein and has a mean chemical composition of $(Cu_{5.92}Ag_{4.21})(Fe_{1.43}Zn_{0.73})(Sb_{3.91}As_{0.11})S_{13}$. The compositions of tetrahedrite from the four stages of vein formation all span a similar range (Table 5). Hackbarth & Petersen (1984) concluded that in most cases, naturally occurring hydrothermal tetrahedrite is heterogeneous in com-

TABLE 7. SEMI-METAL RATIOS & TEMPERATURES FOR COEXISTING SULFOSALTS

VEIN STAGE	PYRA - POLY Sb/(Sb+As)	PYRA - TETR Sb/(Sb+As)	POLY - TETR Sb/(Sb+As)	PYRA-POLY-TETR Sb/(Sb+As)	TEMPERATURE* (°C)
I	0.98 - 0.94	0.98 - 0.97			
I	0.95 - 0.92				
I	0.95 - 0.93				
I	0.97 - 0.91				
I	0.97 - 0.90				
I	0.98 - 0.87				
I	0.95 - 0.81				
I	0.96 - 0.91				
I	0.98 - 0.93	0.98 - 0.95	0.93 - 0.95	0.98 - 0.95 - 0.93	203
I	0.98 - 0.94	0.98 - 0.97	0.94 - 0.97	0.98 - 0.97 - 0.94	203
I	0.98 - 0.93	0.98 - 0.97	0.93 - 0.97	0.98 - 0.97 - 0.93	203
I	0.97 - 0.95				
I	0.97 - 0.95				
I	0.99 - 0.93				218
I	0.98 - 0.90				224
I	0.99 - 0.95				
I	0.96 - 0.93				
I	0.97 - 0.97				
I	0.99 - 0.88				
I	0.98 - 0.88				
I	0.95 - 0.91				
I	0.98 - 0.97				
I	0.98 - 0.92				227
I	0.98 - 0.90				
II		0.99 - 0.99			191
II	0.98 - 0.94				214
II	0.96 - 0.96		0.93 - 0.97		
II	0.97 - 0.89	0.97 - 0.94	0.89 - 0.94	0.97 - 0.94 - 0.89	
II	0.99 - 0.88				230
II	0.96 - 0.94				218
II	0.98 - 0.76				230
II	0.98 - 0.88				232
III		0.99 - 0.99			
III	0.98 - 0.97				215
III	0.98 - 0.96				
III		0.98 - 0.97	0.94 - 0.96		239
IV	0.97 - 0.92				

RATIOS CALCULATED FROM MOLE FRACTIONS. * TEMPERATURES ARE AVERAGES DETERMINED FROM FLUID INCLUSIONS AS REPORTED BY SIMMONS (1986).
ABBREVIATIONS: PYRA PYRARGYRITE, POLY POLYBASITE, TETR TETRAHEDRITE.

position. Microprobe traverses across tetrahedrite grains in this study indicate minor variations in composition, but no distinct pattern of compositional zonation. Tetrahedrite will not be discussed here because numerous studies have documented the compositional variation and crystal structure of tetrahedrite in mineral deposits (Yui 1971, Charlat & Lévy 1974, Wu & Petersen 1977, Miller & Craig 1983, Hackbarth & Petersen 1984, Raabe & Sack 1984, Johnson & Burnham 1985, Johnson *et al.* 1986), and experimental studies with synthetic phases have provided information about their stability fields as a function of temperature (Luce *et al.* 1977, Sack & Loucks 1985).

Solid-solution variation and zonation involving semi-metals and metals

Previous investigations of compositional variation and zonation in sulfosalt solid-solutions in hydrothermal deposits have dealt with tetrahedrite (Boyle 1968, Hickman 1973, Urabe 1974, Wu & Petersen 1977, Hackbarth & Petersen 1984) or geocronite (Birnie & Petersen 1977), but never with

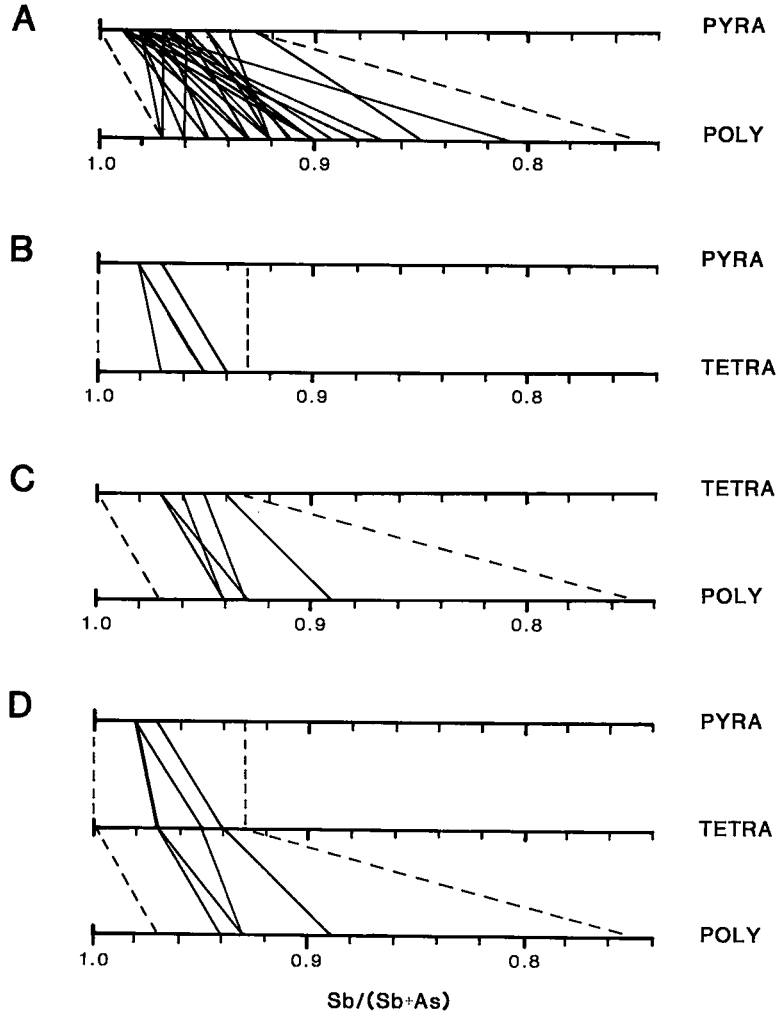

FIG. 9. Compositional tie-lines showing Sb/(Sb + As) values for coexisting sulfosalts in the Santo Niño vein: a) pyrargyrite–polybasite, b) pyrargyrite–tetrahedrite, c) polybasite–tetrahedrite, d) pyrargyrite–polybasite–tetrahedrite. Dashed lines outline the range of Sb/(Sb + As) values for these minerals in the Santo Niño vein. Abbreviations: PYRA pyrargyrite, POLY polybasite, TETRA tetrahedrite.

silver-bearing sulfosalts such as pyrargyrite, polybasite, or stephanite. Compositional variations among sulfosalt minerals are examined using Sb/(Sb + As) and Ag/(Ag + Cu) values (Table 6).

The Sb/(Sb + As) values range from 0.93 to 1.00 for pyrargyrite, from 0.75 to 0.97 for polybasite, from 0.85 to 0.98 for stephanite, and from 0.93 to 1.00 for tetrahedrite. These compositional variations are shown in terms of the quaternary system Ag_2S–Sb_2S_3–As_2S_3–Cu_2S (Fig. 8). As the Sb/(Sb + As) values for the sulfosalt phases do not vary significantly among the paragenetic stages of the Santo Niño vein, *i.e.*, in time, it appears that the composition of the ore-bearing fluids remained relatively constant in concentration of As and Sb.

Compositional zoning of tetrahedrite has been used elsewhere to delineate the direction of fluid flow in hydrothermal deposits, with Sb/(Sb + As) values and silver contents of tetrahedrite both increasing with distance of ascending hydrothermal solutions from an igneous source or center of hydrothermal activity (Wu & Petersen 1977). In the Santo Niño vein, there is no systematic spatial variation in Sb/(Sb + As) values in pyrargyrite, and the limited number of Sb/(Sb + As) values for tetrahedrite and stephanite makes any conclusions relating to their zonation premature. However, the Sb/(Sb + As) values for polybasite, grouped together from all stages and averaged for each location, show a distinct variation from high values in the deeper levels of the vein in the southwest to lower values in the shallow levels to the northeast (Gemmell *et al.* 1988). We propose that the zonation in Sb/(Sb + As) values for polybasite within the Santo Niño vein indicates that the direction of fluid flow was from the deeper portions of the vein in the southwest to shallow levels in the northeast, with a strong lateral component. This would place the source of the solutions close to the deep center of the main Fresnillo mine to the southwest.

In order to determine if there is compositional zonation within the sulfosalts involving the metallic components, Ag/(Ag + Cu) values were examined (Table 6). Ag/(Ag + Cu) values for tetrahedrite are lowest in the southwest portion of the vein on the 425 m level, and increase upward to the shallow levels in the northeast. This pattern indicates that the high-copper (and high-arsenic) tetrahedrite is deposited in the same region of the vein as the arsenic-bearing polybasite. These data suggest that the silver (and antimony) content of the tetrahedrite increases in the same manner within the vein as the antimony content of polybasite. The Ag/(Ag + Cu) values for polybasite, on the other hand, are erratically distributed and do not show any pattern or trend within the vein.

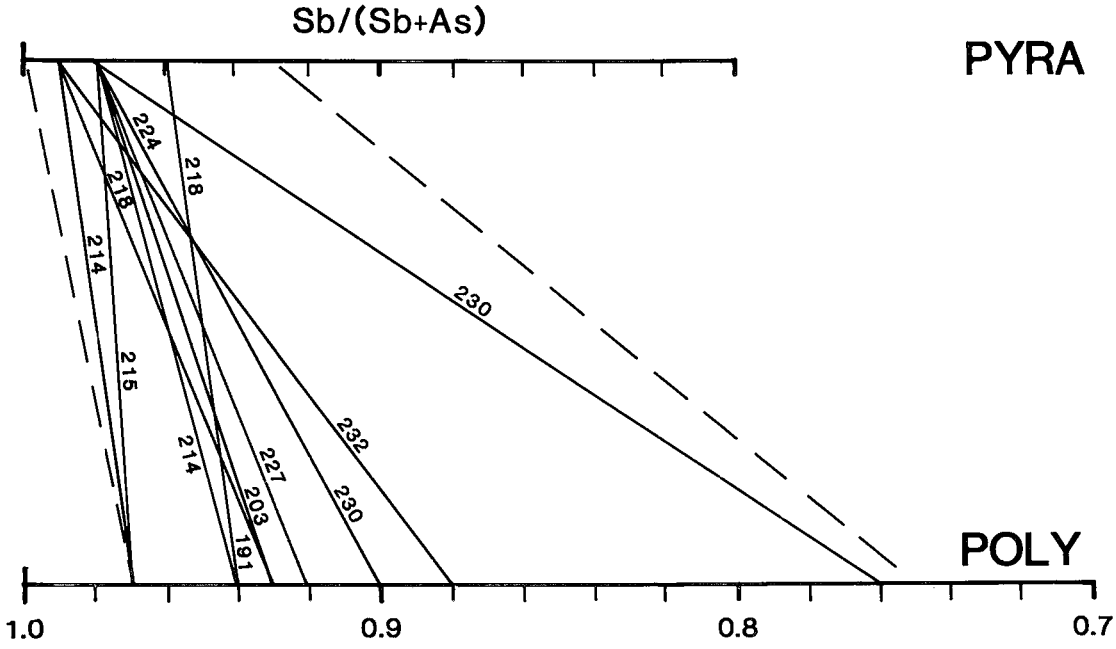

FIG. 10. Relationship between fluid-inclusion temperature and Sb/(Sb + As) tie-lines for coexisting pyrargyrite–polybasite grains. Temperatures, marked on tie lines in °C, are based on fluid-inclusion data in Simmons (1986). Mineral pairs where polybasite has the highest Sb/(Sb + As) value formed at lower temperatures than pairs where polybasite has a low Sb/(Sb + As) value. Dashed lines outline the range of Sb/(Sb + As) values for these minerals in the Santo Niño vein.

Compositional Tie-Lines

The coexistence of pyrargyrite–polybasite and polybasite–tetrahedrite has been reported by Gooddell (1975), but compositional tie-lines between these pairs of minerals and among the other sulfosalts observed in the Santo Niño vein have not been established for natural systems. Pyrargyrite–polybasite, pyrargyrite–tetrahedrite, polybasite–tetrahedrite mineral pairs, and pyrargyrite–polybasite–tetrahedrite mineral triplets occur in physical contact and appear to meet the criteria of simple equilibrium as proposed by Barton *et al.* (1963). Stephanite is a late-stage hypogene mineral and is not considered to have precipitated in equilibrium with pyrargyrite, polybasite and tetrahedrite.

The Sb/(Sb + As) values for coexisting pyrargyrite–polybasite, pyrargyrite–tetrahedrite, polybasite–tetrahedrite, and pyrargyrite–polybasite–tetrahedrite are listed in Table 7. Compositional tie-lines for coexisting pyrargyrite and polybasite for the four stages of vein formation (Fig. 9a) show that polybasite generally has a lower Sb/(Sb + As) value (greater As content) compared to coexisting pyrargyrite, and that many of the tie-lines cross. Birnie & Petersen (1977) suggested that major tie-line cross-overs in such systems could be due to an inhomogeneous sample, to a temperature dependence, or to poor analysis. They proposed that where compositions of the minerals differ by less than two standard deviations, the tie-line cross-overs should not be considered significant. The standard devia-

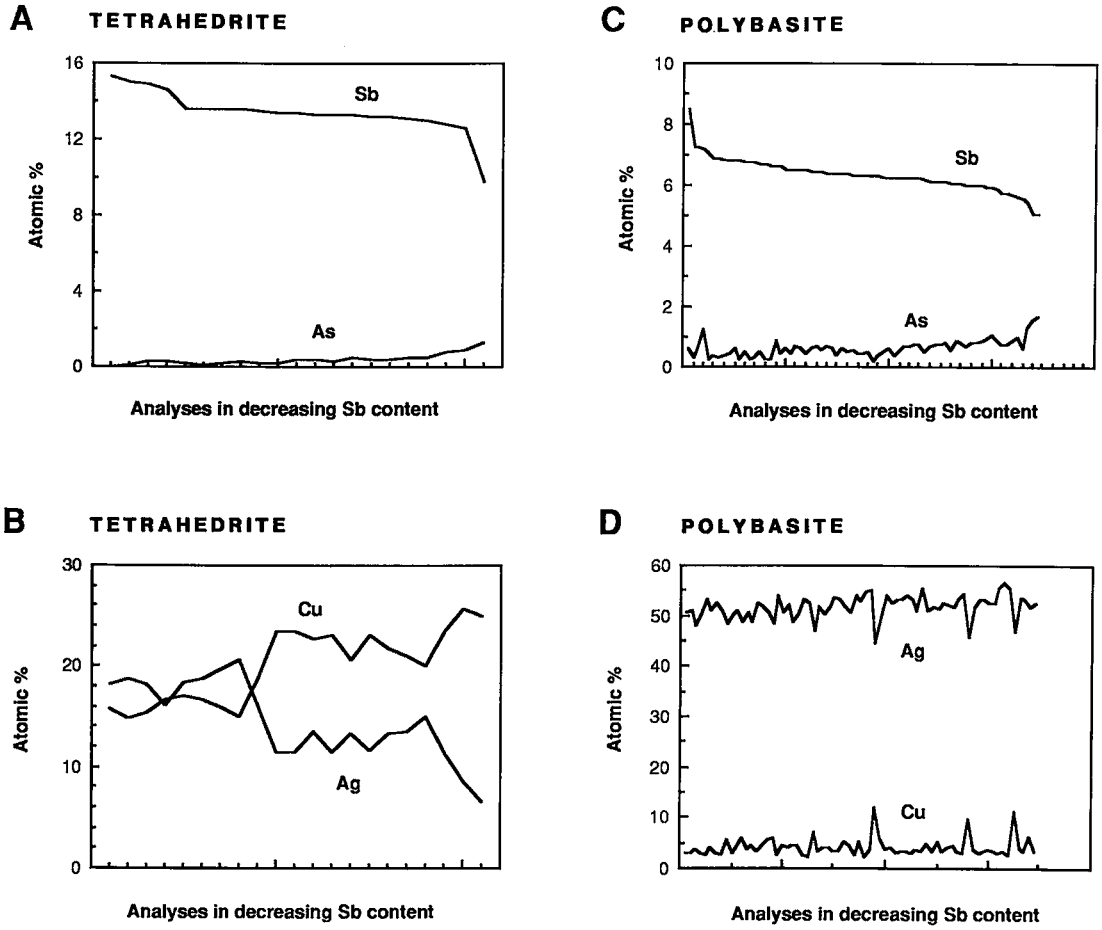

FIG. 11. Semi-metal and metal substitution within tetrahedrite and polybasite from the Santo Niño vein. All elements arranged in order of decreasing antimony content: (a) antimony and arsenic variations in tetrahedrite; (b) silver and copper variations in tetrahedrite; (c) antimony and arsenic variations in polybasite; (d) silver and copper variations in polybasite.

tion associated with the Sb/(Sb + As) values for pyrargyrite and polybasite in the Santo Niño vein are ±0.01 and ±0.04, respectively, and almost all of the tie-lines that cross relate to mineral compositions that differ by less than two standard deviations. However, several pyrargyrite–polybasite pairs do not fit this criterion and produce major tie-line crossovers, suggesting the possibility of a dependence of composition on temperature.

Values of Sb and As in coexisting pyrargyrite and tetrahedrite are shown in Figure 9b. Most pairs have lower Sb/(Sb + As) values in tetrahedrite than in pyrargyrite; in two pairs, the values are equal. Where polybasite and tetrahedrite grains coexist (Fig. 9c), polybasite always has a lower Sb/(Sb + As) value than tetrahedrite.

Several examples of the occurrence of three coexisting sulfosalts were observed. Where pyrargyrite–tetrahedrite–polybasite coexist in equilibrium (Fig. 6c), polybasite has a lower Sb/(Sb + As) value than tetrahedrite, and tetrahedrite has a lower Sb/(Sb + As) value than pyrargyrite (Fig. 9d).

Compositional tie-lines and their relationship to temperature

Goodell (1975) noted that the distribution of compositions among coexisting solid-solutions in the systems Ag_2S–As_2S_3–Cu_2S and Ag_2S–Sb_2S_3–Cu_2S provides potential geothermometers. Feiss (1970) applied a geothermometer using the compositions of enargite–famatinite coexisting with tennantite–tetrahedrite to the ores at Julcani, Peru.

With temperature control provided by the fluid-inclusion studies of gangue and ore minerals (Simmons 1986), the temperature dependence of the phase associations of sulfosalts can be examined. Fluid-inclusion temperatures for the assemblages of coexisting sulfosalts are listed in Table 7. Temperatures of deposition and compositional tie-lines between coexisting pyrargyrite and polybasite are shown on Figure 10. The tie-lines indicate that the Sb/(Sb + As) value of polybasite decreases with increasing temperature, whereas the Sb/(Sb + As) value for pyrargyrite does not change appreciably, suggesting a possible dependence on temperature. Statistical analysis of the temperature variation and the difference between the Sb/(Sb + As) values of coexisting pyrargyrite and polybasite shows a linear relationship, with a correlation coefficient of 0.64 (Gemmell 1986). The temperature associated with individual pairs differs by no more than ± 10°C from the regression line, a value that is well within the limits of other geothermometers applied to ore deposits (Rye 1974). Although the temperature range for these data is limited (200 – 240°C), we suggest that this temperature dependence is a potential geothermometer for epithermal deposits. More ore deposits need to be studied to test the validity and usefulness of this relationship.

Coexisting pyrargyrite–tetrahedrite pairs formed at higher temperatures (Table 7) have lower

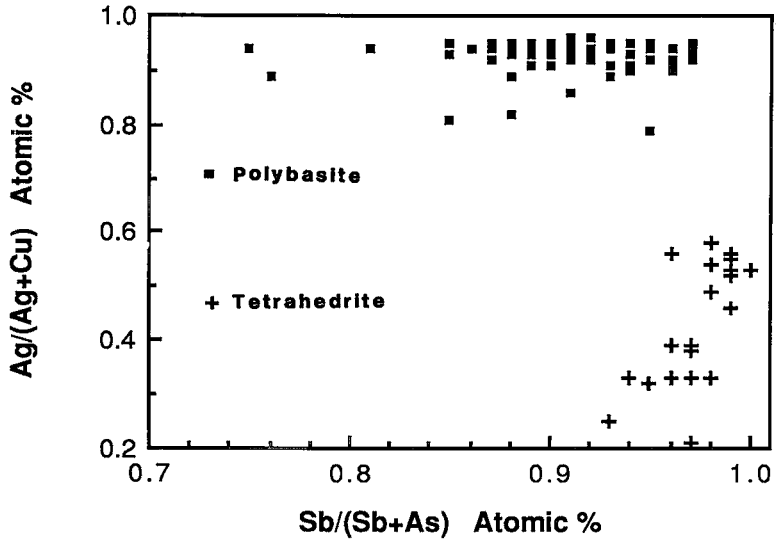

FIG. 12. Compositional variation in tetrahedrite (crosses) and polybasite (solid boxes). These data indicate that there is a coupled relationship between Ag/(Ag + Cu) and Sb/(Sb + As) in tetrahedrite but a noncoupled relationship between Ag/(Ag + Cu) and Sb/(Sb + As) in polybasite.

Sb/(Sb + As) values for both minerals than those formed at lower temperatures, indicating a similar dependence on temperature. However, because of the limited data-base, no conclusions can be drawn concerning the temperature dependence of coexisting polybasite–tetrahedrite mineral pairs.

Interpretation of Systematic Trends in Mineral Composition

A fractional crystallization model, based on the assumption that (Ag–Sb) correlation bands are chords of lines of compositional evolution, was developed by Hackbarth & Petersen (1984) to explain the heterogeneous compositions observed in examples of hydrothermal tetrahedrite. This model suggests that ore fluids are preferentially depleted in copper and arsenic and enriched in antimony and silver, on a single-sample or deposit scale, as deposition proceeds. The fractional crystallization model, however, does not take the compositions of coexisting minerals into consideration.

Miller & Craig (1983) demonstrated the existence of ionic substitution involving antimony and arsenic in the tetrahedrite–tennantite series. They noted that antimony content rises monotonically as arsenic content decreases in the tetrahedrite–tennantite series, demonstrating the diadochy of these two elements. Even though the tetrahedrite compositions from the Santo Niño vein show a very limited range of antimony to arsenic proportions, they do indicate a decrease in Sb as As increases (Fig. 11a). The relationship between silver and copper content, ordered according to decreasing antimony values (Fig. 11b), shows that copper content increases as silver content decreases. This relationship suggests that antimony and arsenic contents in tetrahedrite correlate with silver and copper contents. Miller & Craig (1983) proposed that the positive correlation between silver and antimony is not necessary but permissive (*i.e.*, coupled), since the presence of more antimony in tetrahedrite allows the solid solution to incorporate more silver. Figure 12 indicates a coupled substitution between (Ag–Cu) and (Sb–As) in the tetrahedrite of the Santo Niño vein.

Polybasite contains both (Ag–Cu) and (Sb–As) solid solutions, yet it has received very little attention in the literature. Analysis of the polybasite database, in a manner similar to Miller's & Craig's (1983) treatment of tetrahedrite, points out many interesting similarities and differences between the two minerals. Figure 11c shows antimony content decreasing as arsenic content increases in polybasite, as was the case with tetrahedrite. Although there is a weak sympathetic relationship between silver and copper contents in polybasite (Fig. 11d), there is no extensive substitution, as observed in tetrahedrite. There is no distinct relationship between Ag/(Ag + Cu) and Sb/(Sb + As) in the Santo Niño polybasite samples (Fig. 12); therefore, polybasite seems to display a noncoupled substitution with respect to (Sb–As) and (Ag–Cu).

The pyrargyrite–proustite solid-solution series at Santo Niño shows complete substitution of antimony for arsenic but does not demonstrate any covariation between silver and (Sb–As). The presence of systematic (Sb–As) variation in tetrahedrite but the lack of such in coexisting pyrargyrite led Kortemeier & Burt (1985) to suggest that coupled (Cu–Ag) substitution may be more important in determining (Sb–As) zoning in silver-bearing sulfosalts than fractional crystallization.

In summary, data from the Santo Niño vein indicate that for the coexisting sulfosalt solid-solution series, tetrahedrite shows a coupled substitution with respect to (Sb–As) and (Ag–Cu), polybasite shows a noncoupled substitution with respect to (Sb–As) and (Ag–Cu), and pyrargyrite displays (Sb–As) substitution only. These data suggest that (Sb–As) and (Ag–Cu) zonation in coexisting silver- and silver–copper-bearing sulfosalts is a function of crystal chemistry, not fractional crystallization.

Conclusions

This study of the silver-bearing sulfosalts in the Santo Niño vein has established: (a) the mineral composition and paragenesis of the sulfosalts, (b) the coexistence of members of three separate solid-solution series, (c) the composition and range of semi-metal and metal solid-solutions in each series, (d) systematic changes in semi-metal and metal solid-solution compositions within the vein, which indicate the direction of fluid flow, (e) compositional tie-lines for naturally coexisting pyrargyrite–polybasite, pyrargyrite–tetrahedrite, and polybasite–tetrahedrite mineral pairs and pyrargyrite–polybasite–tetrahedrite mineral triplets, (f) the relationship of compositional tie-lines to temperature, which may provide a potential geothermometer for epithermal deposits, and (g) the depositional systematics of the coexisting sulfosalt phases.

Acknowledgements

This research could not have been completed without the support of Compañía Fresnillo, S.A. de C.V., in particular Dr. G. Ken Lowther, Ing. Gómez de la Rosa, Ing. Gundisalvo Ochoa, Ing. Ricardo Chico, Ing. Enrique García, and the geological staff at Fresnillo. Stuart Simmons, Richard Stoiber, Sam Sawkins, and Eduardo Chico provided valuable discussions. Electron-microprobe analyses were completed with the help of David Lange at Harvard University. This research was funded by the Explorers Club, the Geological Society of America,

the Fairchild Foundation, and the Department of Earth Sciences, Dartmouth College. Thorough editorial reviews were very helpful and are appreciated. Permission of the Compañía Fresnillo, S.A. de C.V. to publish this investigation is gratefully acknowledged.

REFERENCES

ARENAS, P.F. (1860): Descripción geológica y minera del mineral del Fresnillo. *Anales Mexicanos de Ciencias* **1**, 285-346.

BAKER, T.C. (1923): Fresnillo glory-hole mining practice. *Eng. Mining J.* **116**, 931-942.

BARTON, P.B., JR., BETHKE, P.M. & TOULMIN, P., III (1963): Equilibrium in ore deposits. *Mineral. Soc. Am., Spec. Paper* **1**, 171-185.

BIRNIE, R.W. & PETERSEN, U. (1977): The paragenetic association and compositional zoning of lead sulfosalts at Huachocolpa, Peru. *Econ. Geol.* **72**, 983-992.

BOYLE, R.W. (1968): The geochemistry of silver and its deposits. *Geol. Surv. Can. Bull.* **160**.

BYLER, R.E. (1930): Milling practice at Fresnillo. *Mining Mag.* **62**, 137-147.

CHARLAT, M. & LÉVY, C. (1974): Substitutions multiples dans la série tennantite–tetraédrite. *Bull. Soc. fr. Minéral. Cristallogr.* **97**, 241-250.

CHICO, E. (1980): *Descubrimiento de la Veta Santo Niño en Fresnillo, Zacatecas.* Professional thesis, Universidad Nacional Autónoma de México, Mexico City.

CHURCH, J.A. (1907): Proaño, a famous mine of Fresnillo, Mexico. *Eng. Mining J.* **84(2)**, 53-57.

DAMON, P.E., SHAFIQULLAH, M. & CLARK, K.F. (1981): Relations of igneous activity in relation to metallogenesis in the southern Cordillera. *Ariz. Geol. Soc. Digest* **14**, 137-154.

DECSERNA, Z. (1976): Geology of the Fresnillo area, Zacatecas, Mexico. *Geol. Soc. Am. Bull.* **87**, 1191-1199.

DOYLE, J.H. & CHAMBERS, W.F. (1981): ZAF80: an improved quantitative analysis for the Flextran language systems. Golden, Colorado. *Rockwell Internat.* **RFP-3215**, 89 p.

FEISS, G.P. (1970): *Arsenic and Antimony Partitioning between Tennantite–Tetrahedrite and Enargite–Famatinite Series.* Ph.D. thesis, Harvard Univ., Cambridge, Massachusetts.

FRONDEL, C. (1963): Isodimorphism of the polybasite and pearceite series. *Am. Mineral.* **48**, 565-572.

GARCÍA, E., QUEROL, F. & LOWTHER, G.K. (1989): Geología del districto minero de Fresnillo, Zacatecas. *Decade of North American Geology Publ.* (in press).

GEMMELL, J.B. (1986): *The Santo Niño Ag–Pb–Zn vein, Fresnillo District, Mexico: Geology, Sulphide and Sulphosalt Mineralogy, and Geochemistry.* Ph.D. thesis, Dartmouth College, Hanover, N.H.

_____, BIRNIE, R.W. & ZANTOP, H. (1986): Sulphosalt geochemistry of the Santo Niño Ag–Pb–Zn vein, Fresnillo District, Mexico. *Geol. Soc. Am., Abstr. Programs* **18**, 611.

_____, SIMMONS, S.F. & ZANTOP, H. (1988): The Santo Niño silver–lead–zinc vein, Fresnillo District, Mexico. I. Structure, vein stratigraphy, and mineralogy. *Econ. Geol.* **83**, 1597-1618.

_____, ZANTOP, H. & BIRNIE, R.W. (1985): Geology and mineralogy of the Santo Niño Ag–Pb–Zn vein, Fresnillo District, Mexico. *Geol. Soc. Am., Abstr. Programs* **17**, 590.

GOODELL, P.C. (1975): Binary and ternary sulphosalt assemblages in the [Cu_2S–Ag_2S–PbS–As_2S_3–Sb_2S_3–Bi_2S_3] system. *Can. Mineral.* **13**, 27-42.

HACKBARTH, C.J. & PETERSEN, U. (1984): A fractional crystallization model for the deposition of argentian tetrahedrite. *Econ. Geol.* **79**, 448-460.

HALL, H.T. (1965): Structural and compositional relations of pearceite and polybasite. *Am. Geophys. Union Trans.* **46**, 182 (abstr.).

_____ (1967): The pearceite and polybasite series. *Am. Mineral.* **52**, 1311-1321.

HARRIS, D.C., NUFFIELD, E.W. & FROHBERG, M.H. (1965): Studies of mineral sulphosalts. XIX. Selenian polybasite. *Can. Mineral.* **8**, 172-184.

HICKMAN, E.W. (1973): *Zoning in the Ontario mine, Park City district, Utah.* M.S. thesis, Univ. Wisconsin, Madison, Wisconsin.

JOHNSON, M.L. & BURNHAM, C.W. (1985): Crystal structure refinement of an arsenic-bearing argentian tetrahedrite. *Am. Mineral.* **70**, 165-170.

JOHNSON, N.E., CRAIG, J.R. & RIMSTIDT, J.D. (1986): Compositional trends in tetrahedrite. *Can. Mineral.* **24**, 385-397.

KEIGHIN, C.W. & HONEA, R.M. (1969): The system Ag–Sb–S from 600°C to 200°C. *Miner. Deposita* **4**, 157-171.

KORTEMEIER, C.P. & BURT, D.M. (1985): Geochemistry of Ag-sulfosalts from the Tip Top District, central Arizona. *Geol. Soc. Am., Abstr. Programs* **17**, 249.

LANG, B., STEINITZ, G., SAWKINS, F.J. & SIMMONS, S.F. (1988): K-Ar dating studies in the Fresnillo silver district, Mexico. *Econ. Geol.* **83**, 1642-1646.

LUCE, F.D., TUTTLE, C.L. & SKINNER, B.J. (1977): Studies of sulfosalts of copper. V. Phases and phase relations in the system Cu-Sb-As-S between 350° and 500°C. *Econ. Geol.* **72**, 271-289.

MACDONALD, A. J., KRECZMER, M. J. & KESLER, S.E. (1986): Vein, manto, and chimney mineralization at the Fresnillo silver-lead-zinc mine, Mexico. *Can. J. Earth Sci.* **23**, 1603-1614.

MILLER, W.J. & CRAIG, J.R. (1983): Tetrahedrite-tennantite series compositional variations in the Cofer deposit, Mineral District, Virginia. *Am. Mineral.* **68**, 227-234.

MOTOMURA, Y. & YAMAMOTO, S. (1980): Selenian polybasite from the Arakawa No. 3 vein of the Kushikino mine. *Kyushu Univ., Dep. Geol. Sci. Rep.* **13**, 251-257.

PALACHE, C., BERMAN, H. & FRONDEL, C. (1944): *The System of Mineralogy, 7th edition*. John Wiley and Sons, New York, N.Y.

PEACOCK, M.A. & BERRY, L.G. (1947): Studies of mineral sulfosalts. XIII. Polybasite and pearceite. *Mineral. Mag.* **28**, 1-13.

RAABE, K.C. & SACK, R.O. (1984): Growth zoning in tetrahedrite-tennantite from the Hocking mine, Alma, Colorado. *Can. Mineral.* **22**, 577-582.

RUVALCABA-RUIZ, D. (1980): *Geology, Alteration and Fluid Inclusions of the Santa Elena and Santo Niño Fissure Vein Deposits in Fresnillo, Mexico*. M.S. thesis, Colorado State Univ., Golden, Colorado.

_____ (1983): Alteration and fluid inclusions of the Santa Elena and Santo Niño veins in Fresnillo, Mexico. *Geol. Soc. Am., Abstr. Programs* **15**, 346.

_____ & THOMPSON, T.B. (1988): Ore deposits at the Fresnillo mine, Zacatecas, Mexico. *Econ Geol.* **83**, 1583-1596.

RYE, R.O. (1974): A comparison of sphalerite-galena sulfur isotope temperatures with filling temperatures of fluid inclusions. *Econ. Geol.* **69**, 26-32.

SACK, R.O. & LOUCKS, R.P. (1985): Thermodynamic properties of tetrahedrite-tennantites: constraints on the interdependence of the Ag-Cu, Cu-Fe, and As-Sb exchange reactions. *Am. Mineral.* **70**, 1270-1289.

SIMMONS, S.F. (1986): *Physico-chemical Nature of the Mineralizing Solutions for the St. Niño Vein: Results from Fluid Inclusion, Deuterium, Oxygen and Helium Studies in the Fresnillo District, Zacatecas, Mexico*. Ph.D. thesis, Univ. Minnesota, Minneapolis, Minnesota.

_____, GEMMELL, J.B. & SAWKINS, F.J. (1988): The Santo Niño silver-lead-zinc vein, Fresnillo District, Mexico. II. Physical and chemical nature of ore forming solutions. *Econ Geol.* **83**, 1619-1641.

_____ & SAWKINS, F.J. (1986): Physio-chemical nature of the mineralizing solutions of the St. Niño vein, Fresnillo, Zacatecas, Mexico. *Geol. Soc. Am., Abstr. Programs* **18**, 751.

STONE, J.B. (1941): Preliminary description of the Fresnillo District, Zacatecas, Mexico. *Geol. Soc. Am., Abstr. Programs* **52**, 1956-1957.

_____ & MCCARTHY, J.C. (1948): Mineral and metal variations in the veins of Fresnillo, Zacatecas, Mexico. *Mining Technology* **T.P. 1500**, 91-106.

TOULMIN, P., III (1963): Proustite-pyrargyrite solid solutions. *Am. Mineral.* **48**, 725-736.

URABE, T. (1974): Mineralogical aspects of the Kuroko deposits and their implications. *Miner. Deposita* **9**, 309-324.

WU, I.J. & BIRNIE, R.W. (1977): The bournonite-seligmannite solid solution. *Am. Mineral.* **62**, 1097-1100.

_____ & PETERSEN, U. (1977): Geochemistry of tetrahedrite and mineral zoning at Casapalca, Peru. *Econ. Geol.* **72**, 993-1016.

YUI, S. (1971): Heterogeneity within a single grain of minerals of the tetrahedrite-tennantite series. *Soc. Min. Geol. Japan, Spec. Issue* **2**, 22-29.

ZANTOP, H., CHICO, E. & GEMMELL, J.B. (1986): The genetic significance of contrasting metal content, mineral composition and ore textures in veins, mantos and chimneys of the Fresnillo Ag-Pb-Zn deposit, Mexico. *Geol. Soc. Am., Abstr. Programs* **18**, 800.

Received May 25, 1988, revised manuscript accepted March 14, 1989.